Nonlinear Model for Sub- and Superharmonic Motions of a MDOF Moored Structure, Part 1—System Identification

S. Raman
Project Engineer
Skillings-Connolly, Inc.,
5016 Lacey Boulevard S.E., Lacey, WA 98503

S. C. S. Yim
Professor
Coastal and Ocean Engineering Program,
Department of Civil Engineering,
Oregon State University, Corvallis, OR 97331

P. A. Palo
Naval Facilities Engineering Service Center,
1100 23rd Avenue, Port Hueneme, CA 93043

In this first part of a two-part study, the general nonlinear system identification methodology developed earlier by the authors for a single-degree-of-freedom (SDOF) system using the reverse-multi-input/single-output (R-MI/SO) technique is extended to a multi-degree-of-freedom (MDOF), sub-merged, moored structure with surge and heave motions. The physical nonlinear MDOF system model and the formulation of the R-MI/SO system-identification technique are presented. The corresponding numerical algorithm is then developed and applied to the experimental data of the MDOF system using only the subharmonic motion responses to identify the system parameters. The resulting model is then employed in Part 2 for a detailed analysis of both the sub and superharmonic dynamic behavior of the MDOF experimental system and a comparison of the MDOF response results and observations with those of the corresponding SDOF system examined earlier by the authors. [DOI: 10.1115/1.2073208]

Introduction

Nonlinear response behavior, in general, and sub- and superharmonic motions, in particular, of (MDOF) moored structures in the ocean is of great interest to designers of ocean structures. These nonlinear motions may significantly affect the extreme response and fatigue behaviors. They often occur when the dominant wave excitation frequency is near an integer multiple (subharmonic) or rational fraction (superharmonic) of the dominant frequency of the submerged structural system. In order to perform an accurate analysis of these dynamic motions, the parameters of these nonlinear systems need to be determined precisely.

Methods for the parameter identification of linear multi-degree-of-freedom (MDOF) structural systems are well established. Modal superposition and spectral techniques based on the assumption of orthogonality of the normal modes of the system and the subsequent decoupling of the equations using modal vectors are widely used for the analysis and identification of general MDOF system [1]. However, as Rice and Fitzpatrick [2] pointed out, these techniques are limited to linear systems only and not applicable when the systems have significant modal coupling due to damping and/or nonlinearities, (e.g., material and geometry).

The nonlinear identification technique based on the inversion approach of spectral analysis for single-degree-of-freedom (SDOF) systems [3] was extended to the identification of nonlinear parameters of MDOF systems [2]. Bendat et al. [4] independently developed the reverse multiple-input/single-output (R-MI/SO) technique and applied it to several MDOF systems, incorporating nonlinear damping as well as nonlinear stiffness (see also Bendat and Piersol [5]). Recently, R-MI/SO models were developed for offshore engineering applications by Narayanan and Yim [6] and Yim and Narayanan [7] on a SDOF moored structural system; Panneer Selvam and Bhattacharyya [8] on a large floating body; Niedzwecki and Liagre [9] on a distributed parameter marine riser, and Liagre and Niedzwecki [10] on a MDOF minitension-leg platform.

Experiments have been conducted at the O. H. Hinsdale Wave Laboratory at Oregon State University (OSU) on a multipoint moored submerged sphere with SDOF and MDOF configurations subject to wave excitations. Several candidate models were developed in a previous study by the authors [11,12]. With the application on experimental data, the IFF model with the NSND identification algorithm was found to be the most suitable analytical model for the experimental system. Based on the selected model and the identified system parameters, Lin and Yim [13] compared the prediction results with experimental data and Yim and Lin [14] performed a series of analyses on the moored SDOF structural system.

In this study, the IFF-NSND model developed and validated for the SDOF constrained experimental system in the previous study is extended to the MDOF submerged structural system. The IFF-NSND model requires the *a priori* knowledge of the inertia and drag coefficients, C_m and C_d, respectively, for the evaluation of hydrodynamic force on the sphere. To select *a priori* inertia and drag coefficients for our study, we examined the vast library of experimental data on hydrodynamic coefficients for cylinders as a function of the Keulegan–Carpenter number (KC), the Reynolds number (Re), and the roughness parameters from laboratory and field tests [15–19]. For the set of experimental data previously analyzed on the SDOF system, C_m varies between 1.1–1.3 for $5.3\times10^5\leq \mathrm{Re}_F\leq 7\times10^5$ and $4.7\leq \mathrm{KC}_F\leq 6.2$ and 1.3–1.5 for $1.3\times10^5\leq \mathrm{Re}_F\leq 3.7\times10^5$ and $1.2\leq \mathrm{KC}_F\leq 3.3$, and the response was observed to be insensitive to variations in C_d [12]. Using the above range of values for C_m, the general numerical algorithm developed for the MDOF system is applied to the experimental data for subharmonic motions to identify the system parameters and the results are presented.

MDOF System

The MDOF experimental model consists of a submerged moored neutrally buoyant sphere excited by periodic waves with white noise perturbations. The configuration of the model is given in Fig. 1. The restoring force is geometrically nonlinear with the springs attached at an angle of 90°. Springs were used to support the sphere and provide a restoring force. String pots were attached to measure the sphere movement. Pitch motion is observed to be negligible compared to surge and heave motions [20]. With the knowledge of string pot measurements and the distances between

Contributed by the Ocean Offshore and Arctic Engineering Division of ASME for publication in the JOURNAL OF OFFSHORE MECHANICS AND ARCTIC ENGINEERING. Manuscript received September 26, 2004; final manuscript received March 24, 2005. Assoc. Editor: Ge (George) Wang.

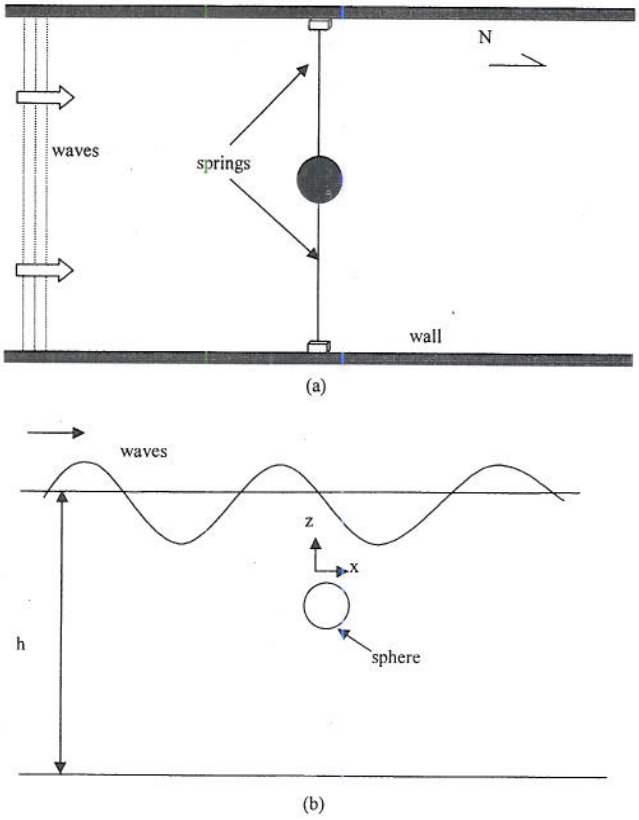

Fig. 1 MDOF experimental setup: (*a*) plan, (*b*) profile view

the sphere and the respective string pots, the readings are converted to surge and heave by two-dimensional geometrical transformations [21].

Governing Equations of Motion

The equations of motion for the SDOF moored structural systems subject to periodic wave excitation with white noise perturbations presented by Narayanan and Yim [11] are extended to the MDOF surge–heave model. By considering surge ($x=x_1$) and heave ($z=x_3$) as the generalized displacement coordinates, assuming that structural damping in the springs and cables can be lumped into equivalent linear structural damping coefficients C_{s1} and C_{s3}, and the geometrically nonlinear restoring force components represented by $R_1(x_1,x_3,t)$ and $R_3(x_1,x_3,t)$, the governing equations of motion for the above mooring system can be written as

$$m\ddot{x}_1(t) + C_{s1}\dot{x}_1(t) + R_1[x_1(t),x_3(t)] = f_1(t) \tag{1a}$$

$$m\ddot{x}_3(t) + C_{s3}\dot{x}_3(t) + R_3[x_1(t),x_3(t)] = f_3(t) \tag{1b}$$

where m=mass of the sphere, $f_1(t), f_3(t)$=excitation force in surge and heave directions, and $\dot{x}_1(t), \dot{x}_3(t), \ddot{x}_1(t), \ddot{x}_3(t)$=sphere velocity and acceleration in surge and heave directions, respectively.

The MDOF mooring restoring forces are derived from the potential function that describes the pretensioned geometrical configuration of a symmetric small body [22]. The resulting coupled expressions in surge and heave are given below:

$$R_1[x_1(t),x_3(t)] = 4Kx_1(t)\left(1 - \frac{l_c}{l(t)}\right), \tag{2a}$$

$$R_3[x_1(t),x_3(t)] = 4Kx_3(t)\left(1 - \frac{l_c}{l(t)}\right), \tag{2b}$$

where $l(t)=\sqrt{d^2+x_1(t)^2+x_3(t)^2}$; K=spring constant, l_c=initial spring length, and d=distance of the center of the sphere from the wall.

The restoring force components in the surge and heave direction are approximated with third-order polynomials obtained using a least-square approximation given by

$$R_1'[x_1(t),x_3(t)] = a_1x_1(t) + a_2x_1^2(t) + a_3x_1^3(t) + c_{12}x_1(t)x_3^2(t), \tag{3a}$$

$$R_3'[x_1(t),x_3(t)] = b_1x_3(t) + b_3x_3^3(t) + c_{21}x_1^2(t)x_3(t). \tag{3b}$$

Note that a square term in the surge direction is included due to its biased (mean offset) response. Numerical comparisons of the polynomials [Eq. (3)] with the geometric model restoring forces [Eq. (2)] showed that the differences between the two expressions are negligible [23]. The normalized errors in both surge and heave directions behave in a similar manner and varies between 0% to 10%. However, the error in the absolute magnitude of the restoring forces at low displacement is mostly insignificant compared to the other terms (i.e., inertia, damping and wave excitation forces) in the dynamic equation of motion [Eq. (1)].

Following the results of the R-MI/SO technique application on the SDOF system [11], an Independent Flow Fields (IFF) model is used to represent the hydrodynamic excitation force on the MDOF model. The components are given by

$$f_1(t) = \rho\,\forall\, C_m\dot{u}_1(t) - m_a\ddot{x}_1(t) + \frac{\rho}{2}A_pC_du_1(t)|u_1(t)| - \frac{\rho}{2}A_pC_{d1}'\dot{x}_1(t) \times|\dot{x}_1(t)| \tag{4a}$$

$$f_3(t) = \rho\,\forall\, C_m\dot{u}_3(t) - m_a\ddot{x}_3(t) + \frac{\rho}{2}A_pC_du_3(t)|u_3(t)| - \frac{\rho}{2}A_pC_{d3}'\dot{x}_3(t) \times|\dot{x}_3(t)| \tag{4b}$$

where $\forall=(\pi/6)D^3$; $\forall=(\pi/6)D^3$; $m_a=(\pi/6)D^3C_a$; u=water particle velocity, ρ=mass density, D=diameter of sphere, C_a =added mass coefficient, C_d'=nonlinear structural damping coefficient, C_m=hydrodynamic inertia coefficient, and C_d =hydrodynamic drag coefficient. For the sphere (with constant projected area) used in this experimental study, the coefficients are taken as the same in both the surge and heave directions and they are given by

$$C_m, C_d = f\left(\mathrm{Re}_F = \frac{u_0D}{\upsilon}, \mathrm{KC}_F = \frac{u_0T}{D}\right) \tag{5a}$$

$$C_a, C_{d1,3}' = f\left(\mathrm{Re}_N = \frac{\dot{x}_0D}{\upsilon}, \mathrm{KC}_N = \frac{\dot{x}_0T_0}{D}\right) \tag{5b}$$

where $u_0, \dot{x}_0$=amplitudes of the water particle and structure velocity, respectively, T and T_0=periods of oscillation of water particle and structure (often equal), υ=viscosity of the fluid, Re =Reynolds number, KC=Keulegan–Carpenter number, subscript "F" refers to the farfield, and subscript "N" to the near field.

Using linear wave theory [24], the deterministic water particle velocities can be written as

$$u_1(t) = \omega a\frac{\cosh k[x_3(t)+s]}{\sinh(kh)}\cos[kx_1(t) - \omega t] \tag{6a}$$

$$u_3(t) = \omega a\frac{\sinh k[x_3(t)+s]}{\sinh(kh)}\sin[kx_1(t) - \omega t] \tag{6b}$$

where $u_1(t), u_3(t)$ are the water particle velocity in the surge and heave directions, respectively, ω=angular velocity, a=wave am-

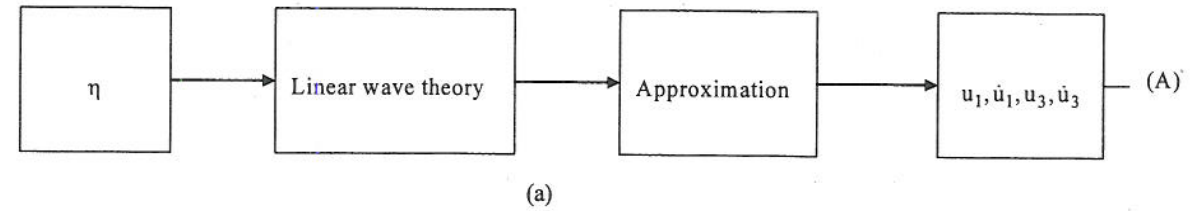

(a)

$$f_{d1}(t) = \frac{1}{2}\rho C_d A_p u_1|u_1| \qquad f_{d1}'(t) = \frac{1}{2}\rho C_{d1}' A_p \dot{x}_1|\dot{x}_1|$$

$$f_{ih1}(t) = C_m \rho \forall \dot{u}_1$$

Fig.1.2a ----- (A)

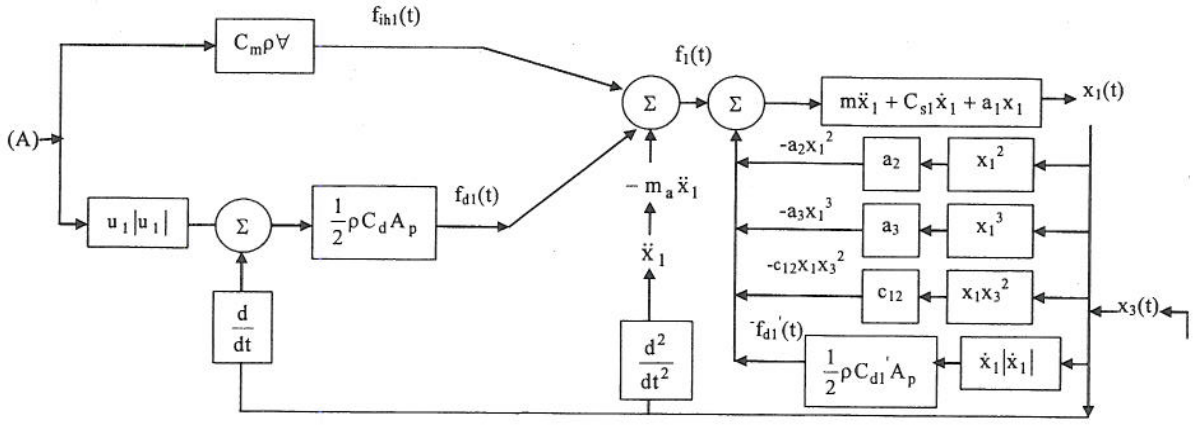

(b)

$$f_{d3}'(t) = \frac{1}{2}\rho C_{d3}' A_p \dot{x}_3|\dot{x}_3| \qquad f_{d3}(t) = \frac{1}{2}\rho C_d A_p u_3|u_3|$$

$$f_{ih3}(t) = C_m \rho \forall \dot{u}_3$$

Fig.1.2a -------- (A)

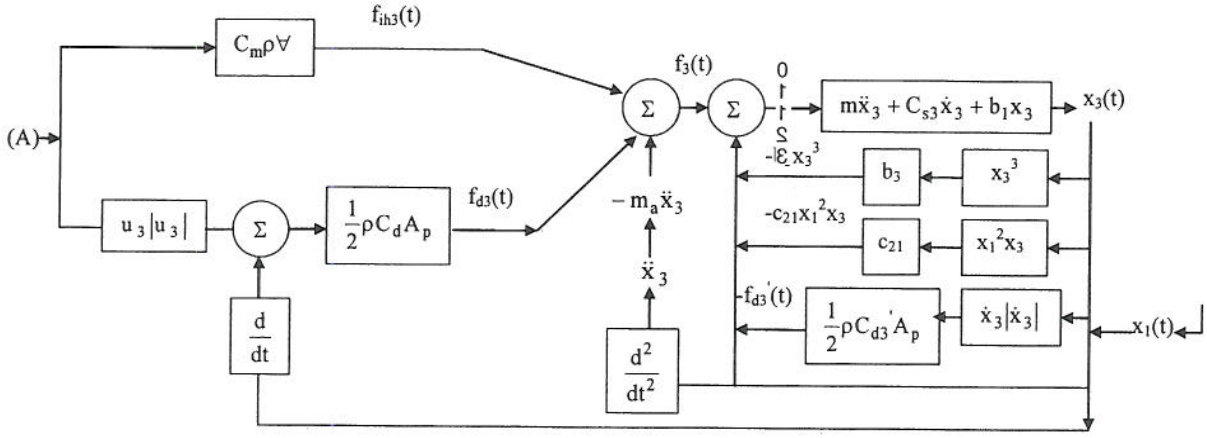

(c)

Fig. 2 Schematic diagram OF the MDOF system: (*a*) system diagram for the calculation of wave velocity and acceleration, (*b*) surge, (*c*) heave

plitude, k=wave number, h=water depth, and s=distance of the instantaneous center of the sphere from the bottom.

The wave excitation containing a periodic component with white noise perturbations may be considered as a randomly perturbed regular wave field. With wave elevation $\eta(t)$ measured for the experiment considered, the water particle velocities, Eqs. (6*a*) and (6*b*), can be approximated as functions of the measure wave elevation and its numerically computed time derivative:

$$u_1(t) = \omega \frac{\cosh k[x_3(t) + s]}{\sinh(kh)} \eta(t) \tag{7a}$$

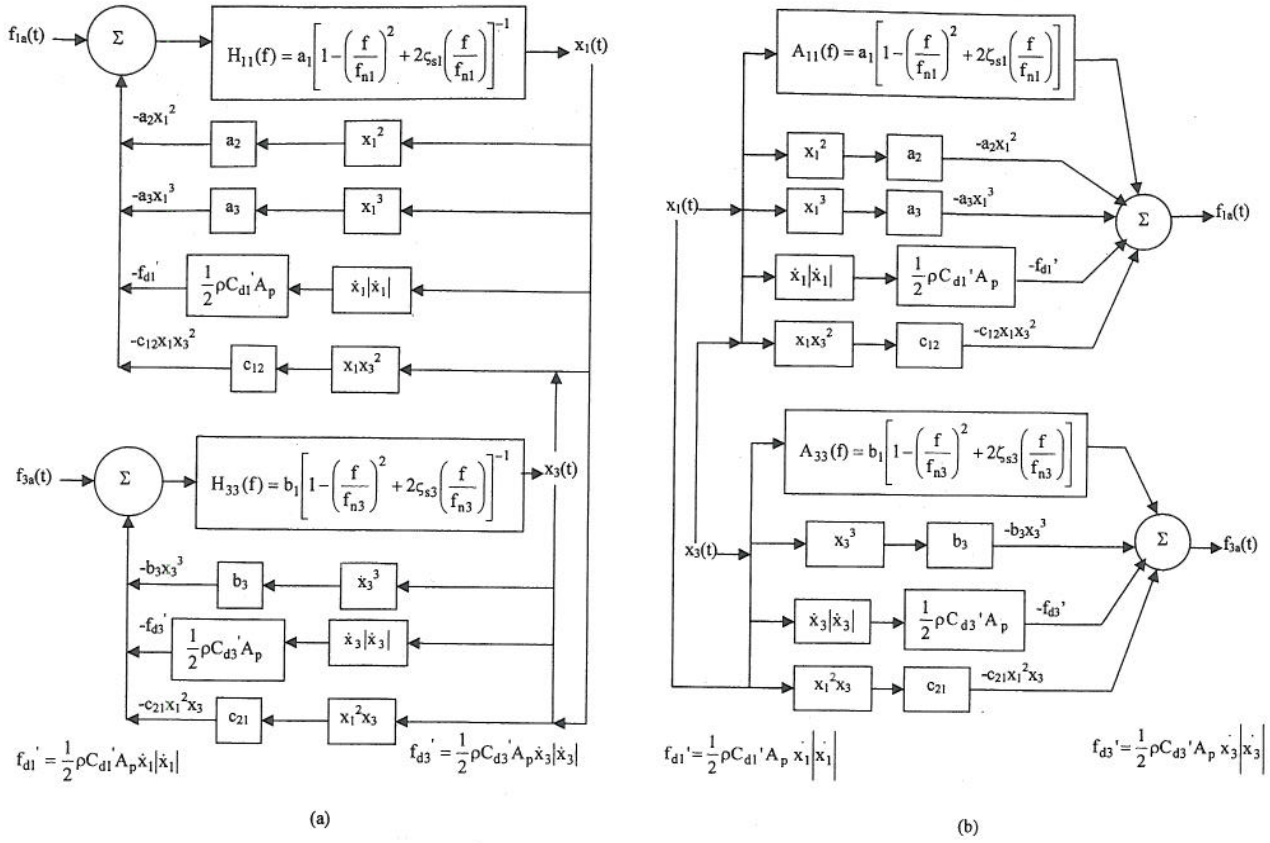

Fig. 3 The nonlinear-structure nonlinearly damped (NSND) model: (*a*) with feedback, (*b*) without feedback

$$u_3(t) = \frac{\sinh k[x_3(t)+s]}{\sinh(kh)}\dot{\eta}(t) \tag{7b}$$

It is assumed that the random perturbations in the excitation are included in $\eta(t)$, given by

$$\eta(t) = a\cos[kx_1(t) - \omega t + \phi] + \xi(t) \tag{8}$$

where $\xi(t)$ is a zero-mean delta-correlated white noise.

The horizontal and vertical, water particle acceleration can also be approximated by functions of the first and second time derivatives of the wave elevation $\eta(t)$ as:

$$\dot{u}_1(t) = \omega_0\frac{\cosh k_0[x_3(t)+s]}{\sinh(k_0h)}\dot{\eta}(t) \tag{9a}$$

$$\dot{u}_3(t) = \frac{\sinh k_0[x_3(t)+s]}{\sinh(k_0h)}\ddot{\eta}(t) \tag{9b}$$

where $\dot{u}_1(t)$ and $\dot{u}_3(t)$ are the water particle accelerations in the surge and heave directions, respectively. The schematic diagram for the MDOF system using the IFF-NSND model as the alternative form of the Morison Equation for representing force is delineated in Figs. 2(*a*)–2(*c*).

Formulation of NSND Model for MDOF System

The R-MI/SO technique can be applied to most nonlinear systems subject to random excitation, irrespective of the nature of the distribution (e.g., Gaussian or non-Gaussian [25]). The relative contribution of the linear and nonlinear system properties, regardless of their frequency dependency or the magnitude of their partial coherence function, can be determined using the R-MI/SO technique.

The nonlinear governing equations of motion for the MDOF NSND model are

$$(m+m_a)\ddot{x}_1(t) + C_{s1}\dot{x}_1(t) + a_1x_1(t) + a_2x_1^2(t) + a_3x_1^3(t) + c_{12}x_3^2(t)x_1(t) + \rho C'_{d1}A_p\dot{x}_1(t)|\dot{x}_1(t)| = f_{1a}(t) \tag{10a}$$

$$(m+m_a)\ddot{x}_3(t) + C_{s3}\dot{x}_3(t) + b_1x_3(t) + b_3x_3^3(t) + c_{21}x_1^2(t)x_3(t) + \rho C'_{d3}A_p\dot{x}_3(t)|\dot{x}_3(t)| = f_{3a}(t) \tag{10b}$$

where

$$f_{1a}(t) = \frac{1}{2}\rho C_dA_pu_1(t)|u_1(t)| + \rho\,\forall\, C_m\dot{u}_1(t) \tag{11a}$$

$$f_{3a}(t) = \frac{1}{2}\rho C_dA_pu_3(t)|u_3(t)| + \rho\,\forall\, C_m\dot{u}_3(t) \tag{11b}$$

Values of the inertia and drag coefficients are assumed to be known *a priori* in order to evaluate the force $f_{1a}(t)$ and $f_{3a}(t)$ given by Eqs. (11*a*) and (11*b*), which are treated as the model input. The system responses, x_1 and x_3, are treated as the model outputs.

Fourier transforming $\mathfrak{I}$ both sides of Eqs. (10*a*) and (10*b*) give the frequency domain relation

$$[a_1 + j(2\pi f)C_{s1} - (2\pi f)^2(m+m_a)]X_{11}(f) + A_{12}(f)X_{12}(f) + A_{13}(f)X_{13}(f) + A_{14}(f)X_{14}(f) + A_{15}(f)X_{15}(f) = F_{1a}(f) \tag{12a}$$

$$[b_1 + j(2\pi f)C_{s3} - (2\pi f)^2(m+m_a)]X_{31}(f) + A_{32}(f)X_{32}(f) + A_{33}(f)X_{33}(f) + A_{34}(f)X_{34}(f) = F_{3a}(f) \tag{12b}$$

where

$$F_{1a}(f) = \mathfrak{I}[f_{1a}(t)], \quad F_{3a}(f) = \mathfrak{I}[f_{3a}(t)] \tag{13a}$$

$$X_{11}(f) = \mathfrak{I}[x_1(t)], \quad X_3(f) = \mathfrak{I}[x_3(t)] \tag{13b}$$

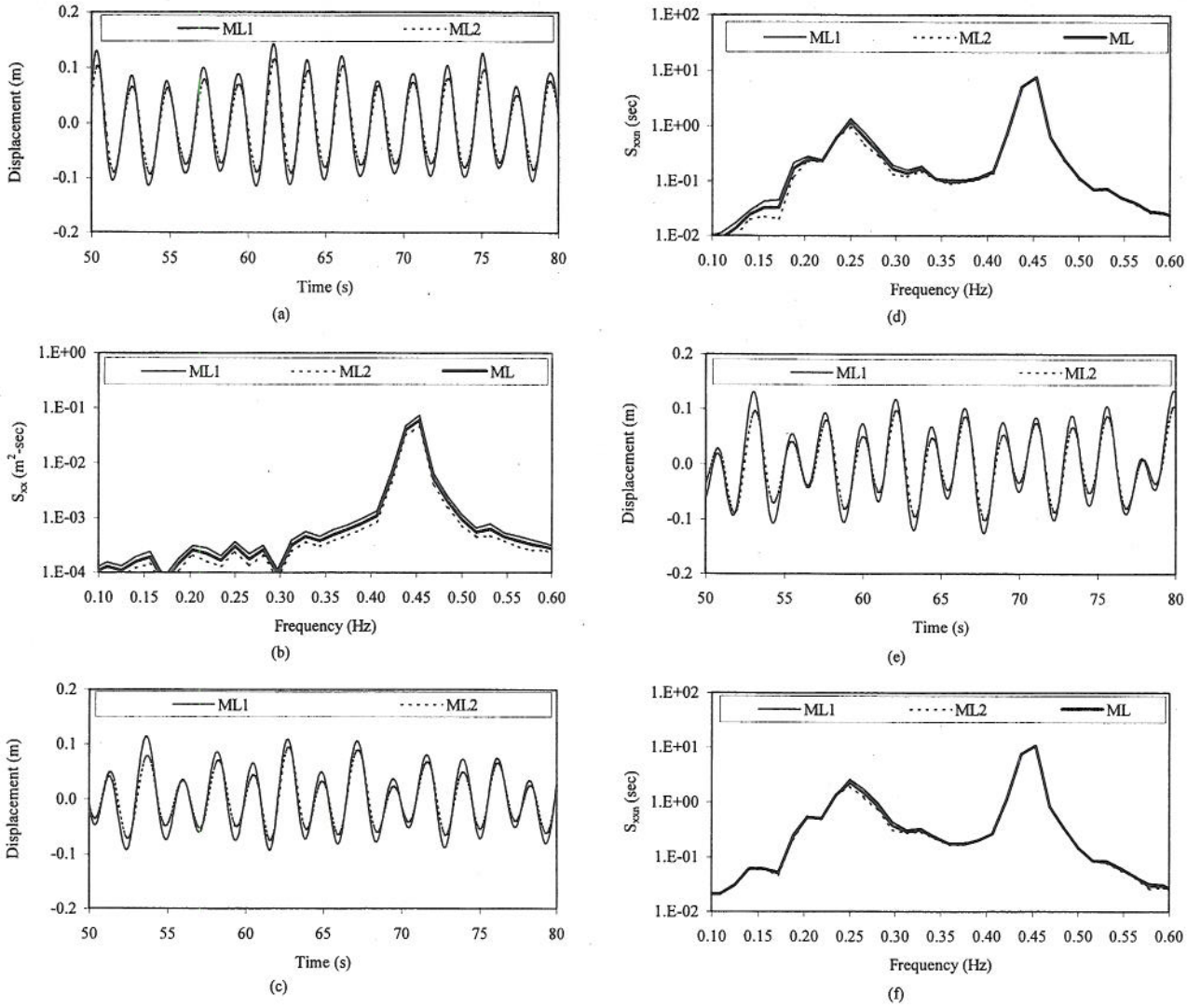

Fig. 4 MDOF experimental data, ML1 and ML2: (*a*) wave time series, (*b*) wave spectra, (*c*) heave time series, (*d*) heave spectra, (*e*) surge time series, (*f*) surge spectra

$$X_{12}(f) = \Im[x_1^2(t)] \tag{13c}$$

$$X_{13}(f) = \Im[x_1^3(t)], \quad X_{32}(f) = \Im[x_3^3(t)] \tag{13d}$$

$$X_{14}(f) = \Im[x_3^2(t)x_1(t)], \quad X_{33}(f) = \Im[x_1^2(t)x_3(t)] \tag{13e}$$

$$X_{15}(f) = \Im[\dot{x}_1(t)|\dot{x}_1(t)|], \quad X_{35}(f) = \Im[\dot{x}_3(t)|\dot{x}_3(t)|] \tag{13f}$$

$$A_{12}(f) = a_2 \tag{13g}$$

$$A_{13}(f) = a_3, \quad A_{32}(f) = b_2 \tag{13h}$$

$$A_{14}(f) = a_4, \quad A_{33}(f) = b_3 \tag{13i}$$

$$A_{15}(f) = \frac{1}{2}\rho C'_{d1}\frac{\pi D^2}{4}, \quad A_{34}(f) = \frac{1}{2}\rho C'_{d3}\frac{\pi D^2}{4} \tag{13j}$$

In the absence of nonlinear terms, $H_{11}(f)$ and $H_{31}(f)$ represent the frequency response functions of an ideal constant parameter linear system that relates the displacement outputs, $x_1(t)$ and $x_3(t)$, to the corresponding force inputs, $f_{1a}(t)$ and $f_{3a}(t)$, respectively. They are given by

$$H_{11}(f) = \frac{X_{11}(f)}{F_{1a}(f)} = [a_1 + j(2\pi f)C_{s1} - (2\pi f)^2(m+m_a)]^{-1}$$
$$= [1 - (f/f_{n1})^2 + 2\zeta_{s1}(f/f_{n1})]^{-1}/a_1 \tag{14a}$$

$$H_{31}(f) = \frac{X_{31}(f)}{F_{3a}(f)} = [b_1 + j(2\pi f)C_{s3} - (2\pi f)^2(m+m_a)]^{-1}$$
$$= [1 - (f/f_{n3})^2 + 2\zeta_{s3}(f/f_{n3})]^{-1}/b_1 \tag{14b}$$

where the natural frequencies, f_{n1}, f_{n3}, and the damping ratios, ζ_{s1}, ζ_{s3}, are defined by

$$f_{n1} = \frac{1}{2\pi}\sqrt{\frac{a_1}{(m+m_a)}}, \quad f_{n3} = \frac{1}{2\pi}\sqrt{\frac{b_1}{(m+m_a)}} \tag{15a}$$

$$\varsigma_{s1} = \frac{C_{s1}}{2\sqrt{a_1(m+m_a)}}, \quad \varsigma_{s3} = \frac{C_{s3}}{2\sqrt{b_1(m+m_a)}} \tag{15b}$$

When nonlinear terms are present, $H_{11}(f)$ and $H_{31}(f)$ relate the displacement outputs to corresponding effective forces, $f_{1e}(t)$ and $f_{3e}(t)$, by

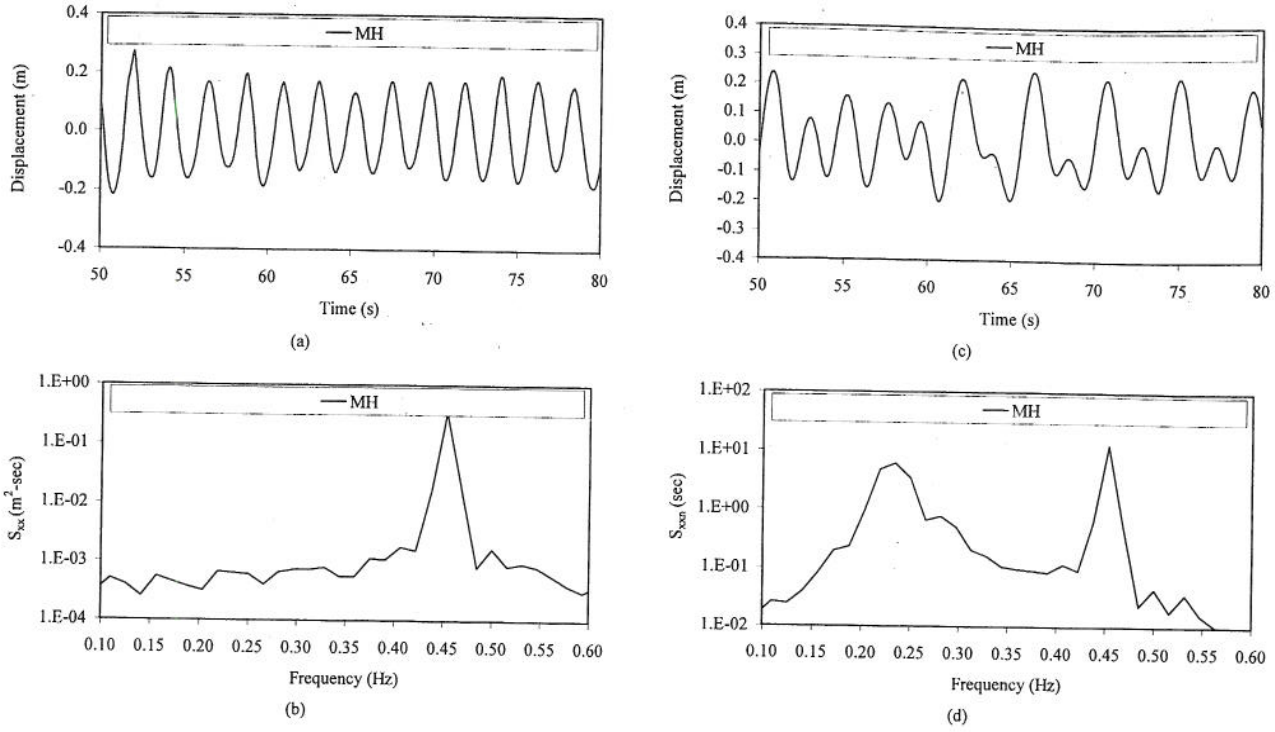

Fig. 5 MDOF experimental data, MH: (*a*) wave time series, (*b*) wave spectra, (*c*) heave time series, (*d*) heave spectra, (*e*) surge time series, (*f*) surge spectra

$$f_{1e}(t) = f_{1a}(t) - a_2x_1^2(t) - a_3x_1^3(t) - c_{12}x_3^2(t)x_1(t) - a_4\dot{x}_1(t)|\dot{x}_1(t)| \tag{16a}$$

$$f_{3e}(t) = f_{3a}(t) - b_3x_1^3(t) - c_{21}x_1^2(t)x_3(t) - b_4\dot{x}_3(t)|\dot{x}_3(t)| \tag{16b}$$

The identification of this system using a standard least-square forward procedure requires a time-consuming iterative approach because of the presence of the nonlinear feedback terms. Because the forward way of analysis is difficult, an alternative reverse dynamic viewpoint is considered [25]. To apply the R-MI/SO technique, the input/output roles are mathematically interchanged (i.e., the strict sense of the equal sign is exploited). The associated Fourier transform relation is given by

$$F_{1a}(f) = A_{11}(f)X_{11}(f) + A_{12}(f)X_{12}(f) + A_{13}(f)X_{13}(f) + A_{14}(f)X_{14}(f) + A_{15}(f)X_{15}(f) \tag{17a}$$

$$F_{3a}(f) = A_{31}(f)X_{31}(f) + A_{32}(f)X_{32}(f) + A_{33}(f)X_{33}(f) + A_{34}(f)X_{34}(f) \tag{17b}$$

$A_{11}(f)$ and $A_{31}(f)$ are defined as the linear impedance functions, which are given by

$$A_{11}(f) = [H_{11}(f)]^{-1} = a_1[1 - (f/f_{n1})^2 + 2j\zeta_{s1}(f/f_{n1})] \tag{18a}$$

$$A_{31}(f) = [H_{31}(f)]^{-1} = b_1[1 - (f/f_{n3})^2 + 2j\zeta_{s3}(f/f_{n3})] \tag{18b}$$

The system gain and phase factors of Eqs. (18*a*) and (18*b*) are given by

$$|A_{11}(f)| = a_1\{\sqrt{[1 - (f/f_{n1})^2]^2 + [2\zeta_{s1}(f/f_{n1})]^2}\} \tag{19a}$$

$$|A_{31}(f)| = b_1\{\sqrt{[1 - (f/f_{n3})^2]^2 + [2\zeta_{s3}(f/f_{n3})]^2}\} \tag{19b}$$

$$\phi_1(f) = \tan^{-1}\left(\frac{2\zeta_{s1}f/f_{n1}}{1 - (f/f_{n1})^2}\right), \quad \phi_3(f) = \tan^{-1}\left(\frac{2\zeta_{s3}f/f_{n3}}{1 - (f/f_{n3})^2}\right) \tag{19c}$$

The minimum gain factor occurs at the resonance frequencies, f_{r1} and f_{r3}, of the system. By determining the maxima of Eqs. (19*a*) and (19*b*), it can be shown that for structures having damping ratio $\zeta_s \leq 0.5$ [26], resonance frequencies are given by

$$f_{r1} = f_{n1}\sqrt{1 - 2\zeta_{s1}^2} \text{ and } f_{r3} = f_{n3}\sqrt{1 - 2\zeta_{s3}^2} \tag{20}$$

The minimum values of the gain factors that occur at resonance are given by

$$|A_{11}(f_{r1})| = a_1(2\zeta_{s1}\sqrt{1 - \zeta_{s1}^2}) \tag{21a}$$

$$|A_{13}(f_{r3})| = b_1(2\zeta_{s3}\sqrt{1 - \zeta_{s3}^2}) \tag{21b}$$

For lightly damped systems, the resonance frequencies and the minimum values of the gain factors can be approximated [25] by

$$f_{r1} \approx f_{n1}, \quad f_{r3} \approx f_{n3}, \quad |A_{11}(f_{r1})| \approx 2a_1\zeta_{s1}, \quad |A_{31}(f_{r3})| \approx 2b_1\zeta_{s3} \tag{22}$$

The physical parameters of the mooring system can therefore be estimated as follows

$$a_1 \approx A_{11}(0), \quad b_1 \approx A_{31}(0) \tag{23a}$$

$$C_a = \frac{m_a}{(\pi/6\rho D^3)} \tag{23b}$$

$$C_{s1} = 2\zeta_{s1}\sqrt{[a_1(m + m_a)]} \approx \frac{|A_{11}(f_{n1})|}{2\pi f_{n1}} \tag{23c}$$

Table 1 Characteristics of the MDOF subharmonic data: (a) wave, (b) identified system parameters (SI units)

(a)

Data	H (m)	KC_F	Re_F	C_m	C_d
ML1	0.29	0.95	9.57e4	1.3	0.1–0.9 (0.5)
ML2	0.23	0.76	7.70e4	1.3	0.1–0.9 (0.5)
ML3	0.47	1.54	1.57e5	1.2	0.1–0.9 (0.5)

(b)

Data	a_1 N/m	a_2 N/m^2	a_3 N/m^3	b_1 N/m	b_3 N/m^3	c_{12} N/m^3	c_{21} N/m^3	$C_{d1,3}$	$\zeta_{1,3}$ %	$f_{n1,3}$ (Hz)
ML1	173.9	405.7	972.4	180.3	1271.9	1568.1	1806.4	1.2	2.5	0.28
ML2	173.9	405.7	1020.7	177.1	1178.5	2273.3	2823.9	0.9	3.1	0.28
MH	180.3	344.5	956.3	173.9	801.8	1912.7	1961.0	0.5	3.2	0.29

$$C_{s3} = 2\zeta_{s3}\sqrt{[b_1(m+m_a)]} \approx \frac{|A_{31}(f_{n3})|}{2\pi f_{n3}} \tag{23d}$$

Last, the fact that the reverse dynamic inputs may be correlated must be addressed. The correlated inputs are replaced with a new set of uncorrelated inputs; this converts the nonlinear model to an equivalent three-input/single-output conditioned linear model [25]. The resulting linear impedance functions yield all the nonlinear system properties given by Eqs. (23). The schematic diagram for the NSND model before and after application of the R-MI/SO technique is given in Figs. 3(*a*) and 3(*b*).

MDOF System Parameter Identification

Three tests, ML1, ML2, and MH (where M stands for the multi-degree-of-freedom system; and L and H for low- and high-amplitude waves, respectively), which yielded subharmonic responses, are employed here for the R-MI/SO parameter identification [20]. These tests were conducted with the same monochromatic wave with period $T=2.2$ s (or frequency $f=0.45$ Hz) but varying wave heights with white noise as the wave excitation. The subharmonic motion responses have a dominant period of 4.4 s (or frequency $f=0.23$ Hz), which is the "natural period" (frequency) of "fundamental mode" vibration of the moored system. The datasets are labeled and grouped according to the wave amplitude. The wave velocity and acceleration are evaluated using the central difference method [27]. The sampling interval used in the experiment is 0.0625 s, which yields a Nyquist frequency of 8 Hz.

Typical segments of the time series and the spectra of the entire record of wave and responses (surge and heave) for the datasets are given in Figs. 4 and 5. The mean spectra, ML, which is the average of ML1 and ML2, are also shown in Figs. 1(*b*), 1(*d*), and 1(*f*). The wave characteristics and the *a priori* quantified coefficients C_m and C_d are given in Table 1(a).

The total number of samples is 8192 (512 s), with subrecord lengths of 1024 and 50% overlapping for the Fourier transforms. By assuming C_m and C_d based on the results of the SDOF system [11], the hydrodynamic force is evaluated using Eq. (4). The R-MI/SO technique is applied on the IFF-NSND model and the system parameters are identified from the experimental data. Using the identified parameters, surge and heave responses are simulated using Eqs. (1), (3), and (4). A typical example of the comparison between the identified and experimental data in the time and frequency domain is given in Fig. 6. The heave and surge response spectral densities, normalized with the variance of corresponding wave data, given by S_{xxn}, which have dimension of seconds, are plotted against frequency, f, in Fig. 6(*b*) and 6(*d*). It can be observed that the simulated responses are comparable to the corresponding experimental responses in both surge and heave directions. The identified system parameters, a_1, a_2, and a_3 (the linear, quadratic, and cubic coefficients of the surge restoring force component), b_1 and b_3 (the linear and cubic coefficients of the heave restoring force component), c_{12} and c_{21} (the coefficients of the surge–heave coupling terms), ζ_1, ζ_3 (the linear damping ratios for surge and heave), $C_{d1,3}$ (the nonlinear drag coefficients) and $f_{n1,3}$ (the structural excitation force components) using the R-MI/SO technique are shown in Table 1(b).

Concluding Remarks

The multipoint moored experimental structure considered in this study has been formulated as a multi-degree-of-freedom (MDOF) surge–heave, submerged, hydrodynamically damped and excited nonlinear oscillator. The restoring force components for the taut elastic mooring cables are geometrically nonlinear and are approximated by third-order polynomials. The nonlinear-structure nonlinearly damped (NSND) model developed and validated for the SDOF configuration in a previous study by the authors is extended here to the MDOF system. Using the measured input wave and output system subharmonic response data and applying

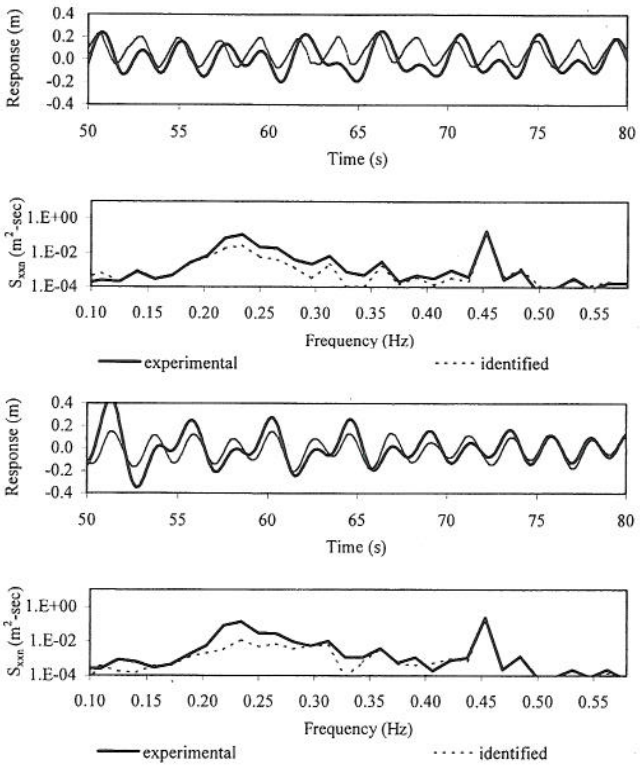

Fig. 6 A comparison between the identified and experimental response for ML: (*a*) (first) heave time series, (*b*) (second) heave spectra, (*c*) (third) surge time series, (*d*) (fourth) surge spectra

the R-MI/SO technique to the model, system parameters that best simulate responses that match the experimental data are identified.

The nonlinear SDOF model presented by the authors in the recent papers is the starting point for the identification of this MDOF system. Based on our previous study of the SDOF system, the independent flow field models the relative-velocity mode for the Morison force formulation. Second, the IFF model with a nonlinear-structure nonlinearly damped (NSND) identification algorithm was selected the most suitable analytical model for this MDOF study [11].

With the basic approach identified, the standard multiple-input/single-output procedures developed for the SDOF nonlinear model were extended to a multi-degree-of-freedom system. Coherence functions were computed that quantify the goodness of fit of the chosen model [23]. Both SDOF and MDOF IFF-NSND models identified system parameters that generate a matching response with that of the experimental data. The formulation of the computational technique is straightforward, simple, and efficient. The standard multiple-input/single-output procedures are incorporated in MATLAB 6.5.1 [28] and once the program has been developed for the SDOF model, as shown in this study, it can be extended to systems with arbitrary degrees of freedom. The larger the degrees of freedom, the more linear and nonlinear transfer functions that yield the linear and nonlinear system parameters would need to be derived and identified. However, the identification of the linear and nonlinear parts of nonlinear models can be implemented using established MI/SO linear procedures and computer programs [27].

Based on the application of the R-MI/SO algorithm to the experimental data, it is shown that the simulated responses using the identified parameters are comparable to the corresponding experimental responses in both surge and heave directions. The validity of the identified parameters of the MDOF based solely on the subharmonic response data will be tested against the measured superharmonic response data in the companion study (Part 2).

Acknowledgments

Financial support from the US Office of Naval Research (Grants No. N00014-92-J-1221 and No. N00014-04-10008) is gratefully acknowledged.

References

[1] Edwins, P. J., 1984, *Model Testing: Theory and Practice*, Research Studies, Letchworth, Hertordshire, England.

[2] Rice, H. J., and Fitzpatrick, J. A., 1991, "The Measurement of Nonlinear Damping on Single Degree-of-Freedom System. Transaction of the American Society of Mechanical Engineers," Trans. ASME, J. Vib. Acoust., **113**, pp. 132–140.

[3] Rice, H. J., and Fitzpatrick, J. A., 1988, "A Generalized Technique for Spatial Analysis of Non-Linearization," Mech. Syst. Signal Process., **2**, pp. 195–207.

[4] Bendat, J. S., Palo, P. A., and Coppolino, R. N., 1992, "A General Identification Technique for Nonlinear Differential Equations of Motion," Probab. Eng. Mech., **7**, pp. 43–61.

[5] Bendat, J. S., and Piersol, A. G., 1993, *Engineering Applications of Correlation and Spectral Analysis*, Wiley, New York.

[6] Narayanan, S., Yim, S. C. S., and Palo, P. A., 1998, "Nonlinear System Identification of a Moored Structural Systems," *Proceedings of the 18th International Offshore and Polar Engineering Conference*, Montreal, Canada, May 24–29 1998, Vol. III, pp. 478–484.

[7] Narayanan, S., and Yim, S. C. S., 2000, "Nonlinear Model Evaluation via System Identification of a Moored Structural System," *Proceedings of the 10th International Offshore and Polar Engineering Conference*, Seattle, USA, 28 May–2 June 2000, Vol. III, pp. 403–409.

[8] Panneer Selvam, R., and Bhattacharyya, S. K., 2001, "Parameter Identification of a Compliant Nonlinear SDOF System in Random Ocean Waves by Reverse-MISO Method," IEEE J. Ocean. Eng., **28**, pp. 1199–1223.

[9] Niedzwecki, J. M., and Liagre, P. Y. F., 2003, "System Identification of Distributed-Parameter Marine Riser Models," IEEE J. Ocean. Eng., **30**, pp. 1387–1415.

[10] Liagre, P. F., and Niedzwecki, J. M., 2003, "Estimating Nonlinear Coupled Frequency-Dependent Parameters in Offshore Engineering," Appl. Ocean. Res., **25**, pp. 1–19.

[11] Naraynan, S., and Yim, S. C. S., 2004, "Modeling and Identification of a Nonlinear SDOF Moored Structure, Part I, Hydrodynamic Models and Algorithm," ASME J. Offshore Mech. Arct. Eng., **126**, pp. 175–182.

[12] Yim, S. C. S., and Narayanan, S., 2004, "Modeling and Identification of a Nonlinear SDOF Moored Structure, Part II, Comparisons and Sensitivity Study," ASME J. Offshore Mech. Arct. Eng., **126**, pp. 183–190.

[13] Lin, H., and Yim, S. C. S., 2005, "An IFF Model for a SDOF Nonlinear Structural System, Part I: Modeling and Comparisons," ASME J. Offshore Mech. Arct. Eng. (in press).

[14] Yim, S. C. S., and Lin, H., 2005, "An IFF Model for a SDOF Nonlinear Structural System, Part II: Analysis of Complex Responses," ASME J. Offshore Mech. Arct. Eng. (in press).

[15] Wang, C. Y., 1965, "The Flow Induced by an Oscillating Sphere," J. Sound Vib., **2**, pp. 257–267.

[16] Hjelmfelt, A. J., Carney, J. F., III, Lee, S. L., and Mockros, L. F., 1967, "Dynamic Response of a Restrained sphere in a Fluid," J. Eng. Mech. Div., **93**, pp. 41–56.

[17] Harleman, D. R. F., and Shapiro, W. C., 1958, "Investigations on the Dynamics of Moored Structures in Waves," M.I.T. Hydrodynamics Lab. Tech. Report No. 28.

[18] Grace, R. A., and Casiano, F. M., 1969, "Ocean Wave Forces on a Sub Surface Sphere," J. Waterw. Harbors Div., Am. Soc. Civ. Eng., **95**, pp. 291–312.

[19] Grace, R. A., and Zee, G. T. Y., 1978, "Further Tests on Ocean Wave Forces on Sphere," J. Waterw., Port, Coastal, Ocean Div., Am. Soc. Civ. Eng., **104**, pp. 83–88.

[20] Yim, S. C. S., Myrum, M. A., Gottlieb, O., Lin, H., and Shih, I.-M., 1993, "Summary and Preliminary Analysis of Nonlinear Oscillations in a Submerged Mooring System Experiment," Ocean Engineering Report No. OE-93-03, Office of Naval Research.

[21] Lin, H., 1994, "Stochastic Analysis of a Nonlinear Ocean Structural System," Ph.D. dissertation. Oregon State University.

[22] Gottlieb, O., and Yim, S. C. S., 1992, "Nonlinear Oscillations, Bifurcations, and Chaos in a Multi-Point Mooring System," Appl. Ocean. Res., **14**(6), pp. 241–257.

[23] Narayanan, S., 1999, "Experimental Analysis of a Nonlinear Moored Structure," Ph.D. dissertation, Oregon State University.

[24] Chakrabarti, S. K., 1987, *Hydrodynamics of Offshore Structures*, Computational Mechanics Publications, London.

[25] Bendat, J. S., 1998, *Nonlinear System Techniques and Application*, Wiley, New York.

[26] Clough, R. W., and Penzien, J., 1993, *Dynamics of Structures*, McGraw-Hill, New York.

[27] Gerald, G. F., and Wheatley, P. O., 1989, *Applied Numerical Analysis*, Addison-Wesley, New York.

[28] MATLAB 6.5.1, The MathWorks, Inc., 1994–2004.